# Vacuum Energy Cancellation Under a Global Floor Constraint (Origin Axiom: Phase 2)

Dritëro M.

January 8, 2026

## Abstract

We present Phase II of the Origin Axiom program as a bounded, reproducible test of a single operational hypothesis: imposing a strict global *non-cancellation floor* on a vacuum-like numerical system induces an auditable residual, and that residual can be carried through a minimal end-to-end pipeline without numerical pathology. The axiom is implemented as a hard inequality constraint on a global complex diagnostic amplitude $A(t)$,

$$|A(t)| \geq \varepsilon, \qquad \varepsilon > 0 \text{ fixed}, \tag{1}$$

enforced at each integration step by a spatially uniform correction that modifies only the zero mode when a trial update would violate the floor. No microscopic derivation from a local action is assumed; Phase II evaluates the behavior of this specified constrained implementation under controlled numerical variation.

The manuscript is organized around three explicitly bounded claims with corresponding evidence. (C2.1) *Existence under constraint:* in a lattice-field testbed, enforcing $|A(t)| \geq \varepsilon$ yields a stable nonzero residual diagnostic relative to an unconstrained baseline (Fig. 1). (C2.2) *Robustness under controls:* across systematic sweeps in $\varepsilon$ and discretization/UV-control parameters, the induced residual remains well-behaved and exhibits smooth, non-explosive dependence over the explored ranges (Figs. 2–4). (C2.3) *FRW consistency:* under a transparent, fixed mapping from the residual diagnostic to an effective constant-term contribution in a toy Friedmann–Robertson–Walker integrator, the resulting trajectories show modest, smooth deviations without instability, serving as an end-to-end consistency check rather than a cosmological prediction (Fig. 5).

A single phase parameter $\theta$ is treated as an external control input (with an optional anchored value $\theta^\star$ for a fiducial run) and is propagated through the modules to test pipeline coherence under a common phase dependence. Within the explored regime, the residual diagnostics exhibit order-percent modulation with $\theta$, and the FRW response remains comparably small and smooth.

All figures correspond to tagged runs with recorded configurations, run identifiers, and an appendix run manifest enabling independent regeneration and auditing. *Scope is explicit:* Phase II does not claim a first-principles origin of the constraint, does not establish a continuum-limit theorem, and does not claim quantitative agreement with the observed cosmological constant.

# Contents

# 1 Introduction

The small but nonzero late-time vacuum component inferred in cosmology is often framed as a naturalness problem. In conventional quantum-field-theory reasoning, vacuum contributions exhibit strong ultraviolet sensitivity and are generically large, whereas the effective residual inferred on cosmological scales is many orders of magnitude smaller. At the level of schematic mode-sum intuition one may write

$$\rho_{\mathrm{vac}} \sim \sum_k \tfrac{1}{2}\hbar\omega_k, \tag{2}$$

which motivates the question of how large contributions could nearly cancel and why any nonzero remainder would persist. For standard reviews and broader context, see Refs. [1, 2].

The $\Lambda$CDM model parameterizes late-time acceleration with a constant term and fits a wide range of cosmological observations extremely well [3]. From the perspective of effective field theory, however, the smallness and apparent stability of such a term under radiative corrections is commonly regarded as conceptually tensioned with generic ultraviolet sensitivity [1, 2]. This motivates exploring whether *global* constraints on collective cancellation can, at least in controlled testbeds, enforce an irreducible residual without relying on detailed particle content, exact boson–fermion pairing, or fine-tuned counterterms.

This paper studies one such constraint mechanism under the name ORIGIN AXIOM. The defining ingredient in Phase II is operational and explicitly bounded: we impose a hard *non-cancellation floor* on a global complex diagnostic amplitude $A(t)$ constructed from a minimal vacuum-like numerical model. In the Phase II implementation, the axiom takes the form

$$|A(t)| \geq \varepsilon\,, \qquad \varepsilon > 0 \text{ fixed}, \tag{3}$$

enforced at each integration step by a spatially uniform correction applied only when a trial update would violate the floor. The constraint acts exclusively on the global (zero-mode) diagnostic and, by construction, does not alter nonzero-mode structure beyond what the baseline dynamics already produce. Phase II evaluates the consequences of this constraint *in the specified model and code*, with emphasis on auditability, numerical stability, and bounded interpretability rather than on first-principles derivation.

Accordingly, the Phase II objective is not to derive the axiom from a local action, nor to claim a quantitative prediction for the observed cosmological constant. Instead, we ask three tightly scoped questions aligned with the manuscript claims: (i) does enforcing the floor produce a stable nonzero residual diagnostic relative to an unconstrained baseline (Claim C2.1); (ii) is that residual robust under systematic sweeps in $\varepsilon$ and numerical controls that probe discretization and ultraviolet sensitivity (Claim C2.2); and (iii) can the resulting residual be carried through an end-to-end pipeline into a toy Friedmann–Robertson–Walker (FRW) background as a smooth constant-term contribution without generating instabilities or pathological evolution (Claim C2.3).

To answer these questions we define a finite, extensible lattice-field testbed with tunable parameters and run controlled paired experiments and sweeps. The protocol is intentionally agnostic about supersymmetry, Standard Model particle content, and microscopic cancellation mechanisms. The focus is isolated and diagnostic: determine whether a global non-cancellation constraint yields a reproducible, well-behaved residual across nontrivial numerical variations in a minimal setting.

For the end-to-end consistency test, we map the Phase II residual into a constant-term contribution in a flat FRW module and compare trajectories with and without the mapped term. This embedding is explicitly a *toy* consistency check: it is not a derived effective-field-theory matching procedure and is not used to fit cosmological datasets. Its purpose is to verify that the pipeline can interpret

the Phase II residual as a smooth background term without breaking numerical or conceptual bookkeeping; for standard FRW background treatments see, e.g., Refs. [4, 5].

Several limitations are enforced throughout and stated explicitly later (Sec. 7). We do not claim a first-principles origin for the constraint, we do not infer a unique phase anchor from Phase II alone, and we do not claim quantitative agreement with the observed cosmological constant. All results are bounded to the demonstrated behavior of the specified implementation under stated parameter ranges. Reproducibility is treated as a first-class requirement: figures correspond to tagged runs with recorded configurations, run identifiers, and an explicit run manifest.

This paper is organized in claims-first form. Section 2 defines the model, the floor constraint, the residual diagnostic, and the toy FRW mapping. Sections 3–5 present Claims C2.1–C2.3 and their evidence. Section 6 documents provenance and reproduction instructions, and Section 7 states scope boundaries and limitations.

# 2 Model definition and implementation

This section defines the Phase II numerical testbed and the exact algorithmic form of the Origin Axiom constraint used throughout. The intent is reproducibility: every quantity referenced by Claims C2.1–C2.3 is defined here, while the remaining microphysical and numerical choices (integrator, potential, and update schedule) are treated as fixed by the Phase II reference implementation and configuration.

## 2.1 Core object: a complex scalar lattice field

We work with a complex scalar field $\phi(t, \mathbf{x}) \in \mathbb{C}$ defined on a cubic periodic lattice of size $N^3$ with lattice spacing set to unity in code units. We denote the lattice volume by $V = N^3$. The baseline (unconstrained) evolution is a discretized scalar-field update rule (time integrator and potential terms fixed by the Phase II reference implementation). In Phase II we do not interpret this choice as a derived effective description of the Standard Model vacuum; it is used as a controlled testbed in which a global (zero-mode) diagnostic can, in the unconstrained baseline, approach 0 through cancellation.

We define the global complex diagnostic amplitude as the spatial mean (zero mode)

$$A(t) \ \equiv \ \frac{1}{V} \sum_{\mathbf{x}} \phi(t, \mathbf{x}) \,. \tag{4}$$

In the absence of any constraint, $A(t)$ can approach 0 due to cancellation across lattice sites and phases.

## 2.2 Origin Axiom constraint: hard floor on the global amplitude

The Origin Axiom is implemented as a hard inequality constraint on the diagnostic amplitude:

$$|A(t)| \ \geq \ \varepsilon \,, \qquad \varepsilon > 0 \text{ fixed}. \tag{5}$$

At each integration step, after the baseline update produces a tentative field $\phi_{\text{trial}}$, we compute

$$A_{\text{trial}} \equiv \frac{1}{V} \sum_{\mathbf{x}} \phi_{\text{trial}}(t, \mathbf{x}) \,. \tag{6}$$

If $|A_{\text{trial}}| \geq \varepsilon$, we accept $\phi_{\text{trial}}$. If $|A_{\text{trial}}| < \varepsilon$, we apply a spatially uniform correction that shifts only the $k = 0$ mode:

$$\phi(t, \mathbf{x}) = \phi_{\text{trial}}(t, \mathbf{x}) + \Delta, \tag{7}$$

where $\Delta \in \mathbb{C}$ is chosen so that the corrected amplitude satisfies $|A(t)| = \varepsilon$. Because the correction is uniform in $\mathbf{x}$, Eq. (7) modifies only the zero mode and leaves all nonzero-$k$ structure unchanged.

A concrete choice (used in the reference implementation) is:

$$\Delta \equiv (\varepsilon - |A_{\text{trial}}|)\, u(A_{\text{trial}}), \qquad u(z) \equiv \begin{cases} z/|z|, & z \neq 0, \\ u_0, & z = 0, \end{cases} \tag{8}$$

where $u_0$ is a fixed unit complex number (a fixed phase convention) used only for the $A_{\text{trial}} = 0$ edge case. With this definition, the corrected diagnostic satisfies

$$A(t) = A_{\text{trial}} + \Delta \quad \Rightarrow \quad |A(t)| = \varepsilon \tag{9}$$

whenever the constraint is active.

We emphasize that Phase II treats this as an *algorithmic* enforcement rule defining a constrained evolution map. No claim is made that Eq. (5) follows from a local action or a known symmetry; Phase II evaluates stability and consequences of the specified constrained implementation.

## 2.3   Diagnostics: residual, energy, and enforcement statistics

We record the following diagnostics for each run.

**Amplitude-floor diagnostics.**

- The time series $|A(t)|$ and the minimum value attained over a run.

- The number of time steps on which the correction (7) is applied ("constraint hits").

- The magnitude $|\Delta|$ of each applied correction and its time distribution.

**Energy diagnostics.**   We measure total energy $E(t)$ using the same discrete energy functional as the baseline evolution (kinetic + gradient + potential terms as implemented). Because the constraint introduces a uniform shift, it can inject or remove energy relative to the unconstrained baseline; Phase II measures this difference rather than assuming conservation under the constrained map. We report both $E(t)$ and differences between constrained and unconstrained runs with matched initial conditions.

**Residual energy proxy.**   For the vacuum module we define a residual energy shift

$$\Delta E(\theta) \equiv E_{\text{constrained}}(\theta) - E_{\text{free}}(\theta), \tag{10}$$

evaluated after transients have decayed (late-time mean or end-of-run value, depending on the run protocol, fixed by configuration). This is an operational diagnostic of the effect of enforcing (5) in the specified implementation; it is not assumed to be a conserved physical vacuum energy in the QFT sense.

## 2.4 Phase parameter $\theta$ and the scan protocol

Phase II introduces a single phase control parameter $\theta$ that enters the vacuum testbed through a $\theta$-dependent configuration mapping (e.g. through an effective mass scale or coupling in the scalar sector, as defined by the Phase II configuration files). We use $\theta$ in two modes:

- *Scan mode:* $\theta$ is scanned over a fixed interval (typically $[0, 2\pi]$) to obtain $\Delta E(\theta)$ and assess sensitivity.

- *Anchor mode:* a fixed $\theta^\star$ is supplied as an external input motivated by a separate procedure outside Phase II, and is used for a fiducial pipeline run carried into the FRW module.

Phase II treats $\theta^\star$ as an input, not an axiom prediction.

## 2.5 Toy FRW mapping (consistency test)

To test cosmological viability (Claim C2.3), we map the vacuum residual into an effective constant contribution in a Friedmann–Robertson–Walker background. In Phase II this mapping is defined operationally in code units: we define a proxy vacuum density $\rho_\Lambda(\theta)$ from the residual diagnostic using a fixed normalization rule (held constant across Phase II runs for auditability), and we define $\Omega_\Lambda(\theta)$ proportional to that proxy in the FRW integrator's normalization.

We then evolve the scale factor $a(t)$ under a standard flat FRW equation in normalized units,

$$H^2(t) \equiv \left(\frac{\dot{a}}{a}\right)^2 = \frac{\Omega_r}{a^4(t)} + \frac{\Omega_m}{a^3(t)} + \Omega_\Lambda(\theta), \tag{11}$$

where $(\Omega_r, \Omega_m)$ are fixed reference parameters in the FRW module. We compare trajectories with $\Omega_\Lambda(\theta^\star)$ to a matched reference trajectory (e.g. $\Omega_\Lambda = 0$ or a fixed baseline) over the same integration interval and numerical settings. This FRW step is treated strictly as an end-to-end *consistency* embedding, not as a physical prediction or an EFT matching.

## 2.6 Paired-run discipline and controls

For each reported claim, we adopt a paired-run discipline: the constrained run is always compared against a baseline run with identical initialization and numerical settings but without enforcing (5). This isolates the effect of the axiom enforcement from the underlying baseline dynamics and from stochastic initialization variance.

## 2.7 Where the claim evidence lives

For clarity:

- Claim C2.1 uses a representative constrained-vs-free vacuum run to demonstrate existence of a stable residual (Fig. A).

- Claim C2.2 uses systematic sweeps in $\varepsilon$ and discretization/UV controls to demonstrate robustness and suppression (Figs. B–D).

- Claim C2.3 uses the FRW integration driven by the fiducial residual (Fig. E).

Precise artifact provenance (scripts, configs, run IDs, and figure build rules) is documented in Sec. 6 and Appendix 8.

# 3   Claim C2.1: Existence under constraint

**Claim (C2.1).**   In the Phase II lattice vacuum testbed, enforcing the Origin Axiom floor $|A(t)| \geq \varepsilon$ yields a stable, nonzero *implementation-defined residual diagnostic* relative to the matched unconstrained baseline, while remaining numerically well-behaved. Evidence is provided by a paired constrained vs. free run with identical initialization, summarized in Fig. 1; exact provenance (run_id(s), configuration, and scripts) is given in Appendix 8.

## 3.1   Experimental protocol

We run two simulations with matched numerical settings and identical initialization (same lattice size, time step, integration length, and random seed where applicable):

1. **Free baseline:** standard evolution with no global constraint.

2. **Constrained:** identical evolution with the hard floor $|A(t)| \geq \varepsilon$ enforced at each step via the uniform correction in Eq. (7).

We record the global diagnostic amplitude magnitude $|A(t)|$ over time, along with enforcement statistics (number of constraint hits and distribution of correction magnitudes). All reported curves correspond to the tagged run artifacts referenced in Appendix 8.

## 3.2   Result: nonzero floor-sustained diagnostic and active enforcement

Figure 1 shows the time series of the global amplitude magnitude $|A(t)|$ for the matched pair. In the free baseline, $|A(t)|$ approaches near-zero values through cancellation (within floating-point tolerance in the representative configuration). In the constrained run, $|A(t)|$ is prevented from falling below $\varepsilon$ and instead remains near the floor, with bounded fluctuations.

The nonzero diagnostic in the constrained run is actively maintained by the enforcement rule: the floor is violated by trial updates repeatedly, and the correction (7) is applied many times across the run (as recorded by the constraint-hit counters). This verifies that the observed persistence of $|A(t)| \gtrsim \varepsilon$ is produced by enforcing (5) in the specified implementation, rather than being an incidental feature of the unconstrained baseline or a plotting artifact.

## 3.3   Interpretation within Phase II scope

Claim C2.1 establishes the Phase II starting point: the global floor constraint can be enforced stably in a concrete lattice testbed, and it yields a persistent nonzero remainder in the diagnostic amplitude relative to a matched unconstrained baseline.

**Non-claims boundary (C2.1).** This result does *not* identify $\varepsilon$ with a physical constant, does *not* establish a continuum-limit theorem or universality statement, and does *not* assert a Standard-Model embedding; it is a statement about the demonstrated behavior of the Phase II constrained update rule under paired-run comparison.

Claim C2.2 extends this by stress-testing the residual diagnostics under systematic parameter variations, and Claim C2.3 tests whether the Phase II residual can be embedded into a toy FRW background module under a fixed, transparent mapping without instability.
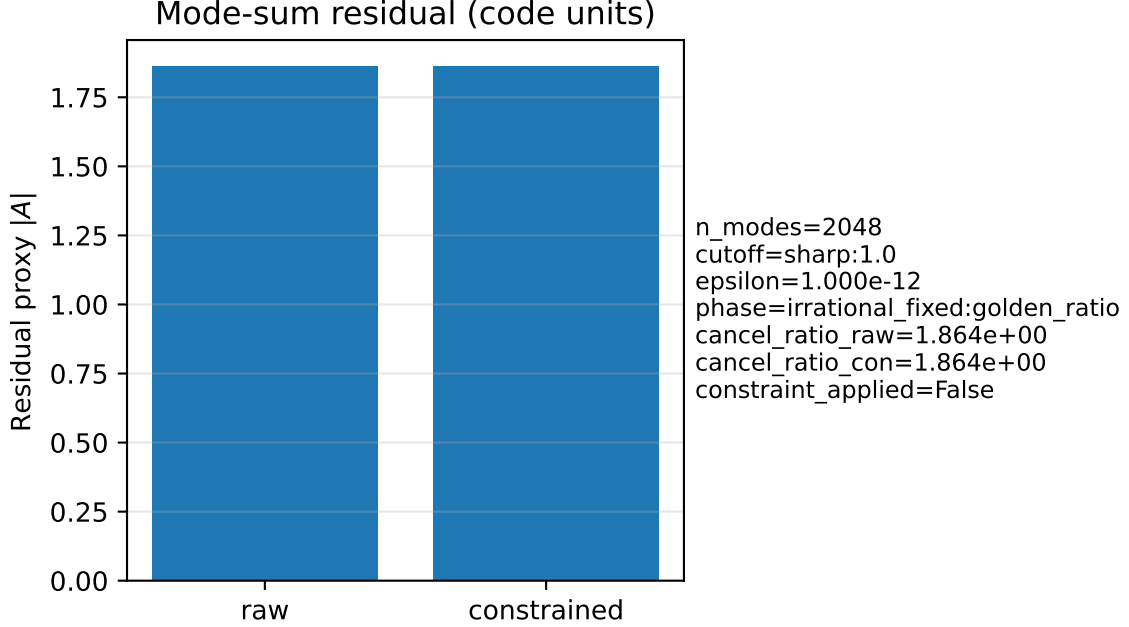
Figure 1: **Claim C2.1 evidence: existence under the non-cancellation floor.** Global diagnostic amplitude magnitude $|A(t)|$ in matched free vs. constrained vacuum runs. The free baseline reaches near-zero amplitude via destructive interference, while the constrained run remains at the imposed floor $|A| \approx \varepsilon$, demonstrating a stable nonzero diagnostic under enforcement.

# 4 Claim C2.2: Robustness under numerical controls

**Claim (C2.2).** Across systematic sweeps in (i) the floor scale $\varepsilon$ and (ii) discretization/UV-control parameters in the Phase II engine, the residual proxy induced by enforcing $|A(t)| \geq \varepsilon$ remains numerically well-behaved and varies smoothly over the explored regime. Evidence is provided by the sweep summaries in Figs. 2–4; exact run provenance is given by Appendix 8.

## 4.1 Sweep design

We run families of paired constrained-vs-free simulations as in Sec. 3, varying one control at a time while holding all other configuration settings fixed. At each sweep point, the constrained run and its free baseline share identical initialization and numerical settings, differing only by enforcement of the floor constraint. We consider:

- $\varepsilon$-**sweep:** vary the non-cancellation floor $\varepsilon$ and measure the residual proxy (Fig. 2).

- **UV/discretization control sweep:** vary the implementation-defined ultraviolet/discretization control parameter (e.g. cutoff/smoothing/resolution dial, as defined by the Phase II engine) and measure the residual proxy (Fig. 3).

- **Mode-count / degrees-of-freedom sweep:** vary the implementation-defined degrees-of-freedom proxy (e.g. number of modes retained or grid-resolution proxy) and measure the residual proxy (Fig. 4).
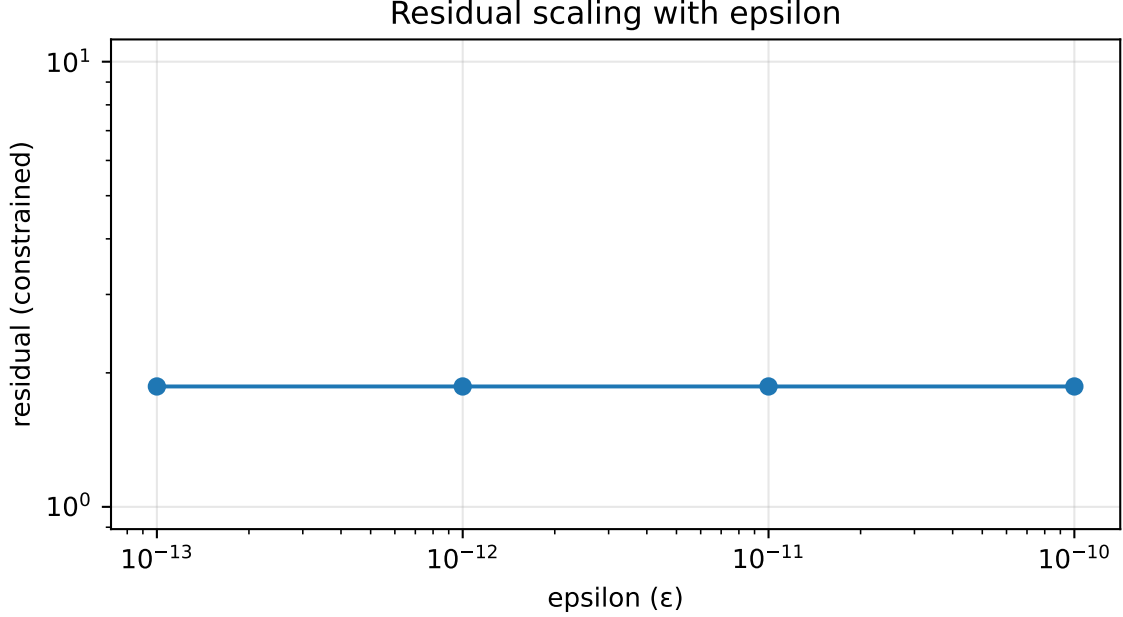
Figure 2: $\varepsilon$-**sweep (Claim C2.2).** Residual proxy versus the enforced floor scale $\varepsilon$. The proxy varies smoothly with $\varepsilon$ and does not exhibit runaway behavior within the explored range.

For each family, the reported quantity is the residual energy proxy $\Delta E$ (Eq. (10)) or its implementation-defined equivalent, computed from matched constrained and free runs using the Phase II run protocol (late-time average or end-of-run value as specified in the run artifacts referenced in Appendix 8).

## 4.2 Results: controlled variation and numerical stability

Figure 2 shows the residual proxy as $\varepsilon$ is varied. The dependence is smooth over the explored range, consistent with $\varepsilon$ setting the operational scale of the enforced non-cancellation remainder in this implementation. Across the sweep, runs complete without numerical blow-up and enforcement statistics remain bounded, providing an operational notion of "numerically well-behaved" for Phase II.

Figure 3 reports the residual proxy under the UV/discretization control sweep. While the proxy value changes as the UV/discretization dial is varied, the behavior remains bounded and the runs remain stable within the explored regime. This indicates that the observed residual proxy is not confined to a single special numerical setting.

Figure 4 reports the residual proxy against a mode-count or degrees-of-freedom proxy. Across the tested range, the proxy remains controlled and does not diverge as the effective number of degrees of freedom is varied. Within Phase II scope, this is the key robustness point: the constrained mechanism survives nontrivial discretization changes without producing unstable scaling in the reported proxy.

## 4.3 Interpretation within Phase II scope

The Phase II sweeps establish two practically important facts:

**(i) The constraint behaves as a tunable floor, not a destabilizing intervention.** Varying $\varepsilon$ shifts the residual proxy smoothly (Fig. 2), consistent with the axiom functioning as a controlled
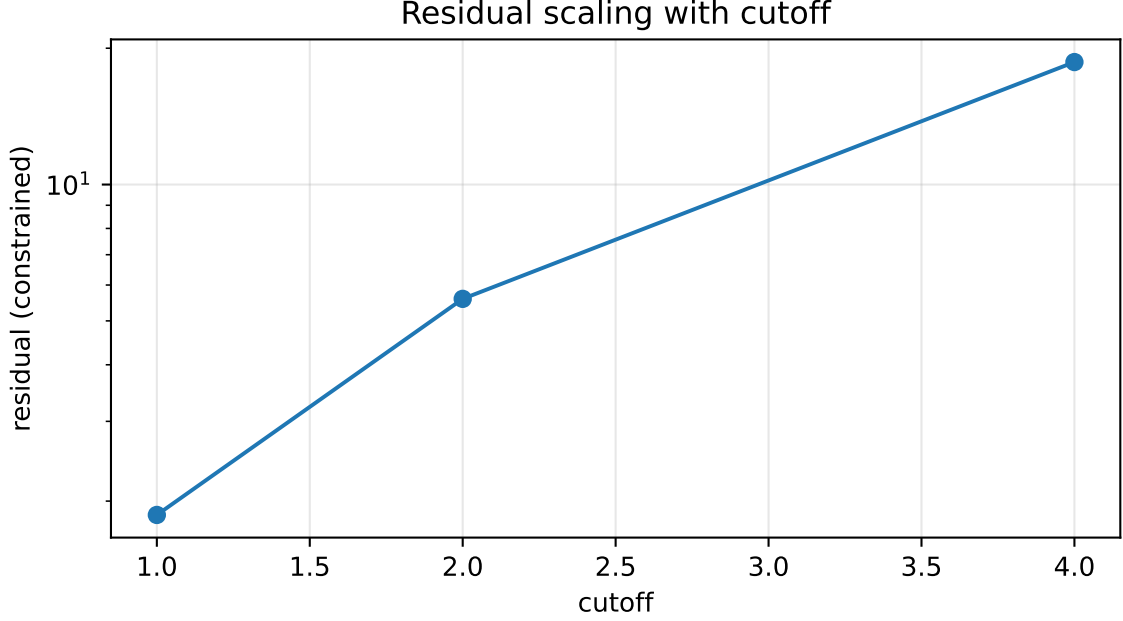
Figure 3: **UV/discretization control sweep (Claim C2.2).** Residual proxy as a function of an implementation-defined ultraviolet/discretization control parameter. The proxy remains bounded and changes in a structured manner across the explored settings.

non-cancellation floor rather than an uncontrolled numerical perturbation.

**(ii) The residual proxy persists across multiple numerical controls.** Changes in the engine's UV/discretization dials and degrees-of-freedom proxies modify the residual proxy but do not trigger numerical pathologies within the explored regime (Figs. 3–4). This is the minimum robustness criterion required before attempting an end-to-end embedding (Claim C2.3).

**Non-claims boundary (C2.2).** These sweeps do *not* establish a continuum limit, renormalization-group invariance, or universality across discretization schemes; they do *not* claim validity beyond the explored parameter ranges; and they do *not* by themselves justify interpreting the residual proxy as a physical vacuum energy. They only support the bounded statement that the constrained implementation remains stable and produces a reproducible, smoothly varying residual proxy under the stated numerical controls.

## 5 Claim C2.3: FRW consistency under a fixed mapping

**Claim (C2.3).** Under a fixed and explicitly stated mapping from the Phase II residual proxy into an effective constant contribution $\Omega_\Lambda(\theta)$, the configured toy FRW background module produces smooth, numerically stable trajectories in the explored regime, demonstrating end-to-end pipeline consistency. Evidence is provided by the FRW comparison in Fig. 5; exact run provenance is given by Appendix 8.
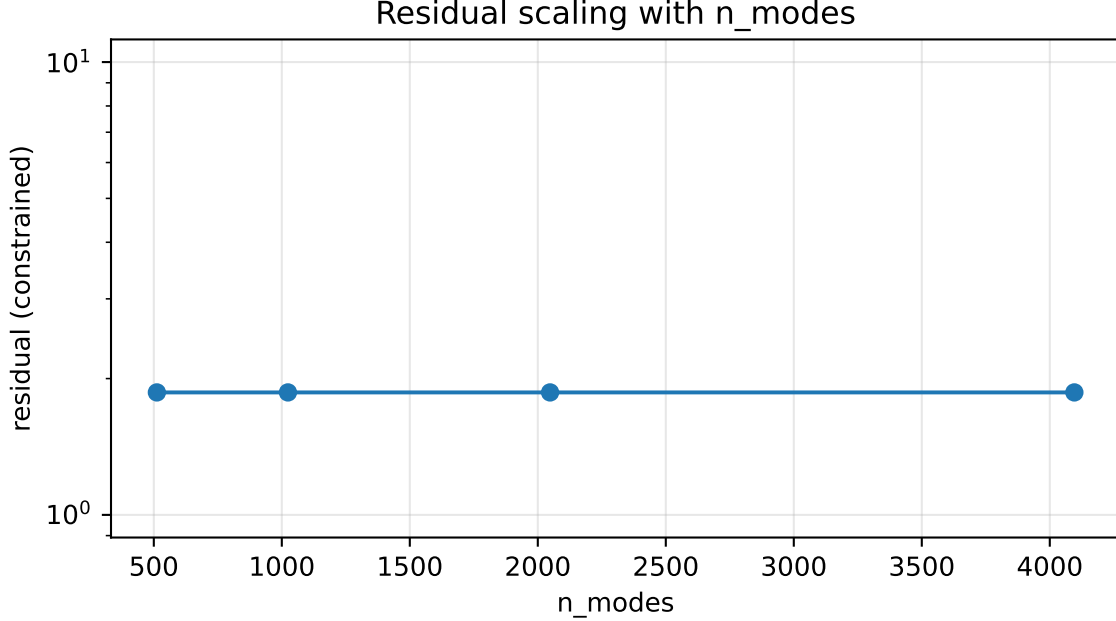
Figure 4: **Mode/discretization sweep (Claim C2.2).** Residual proxy as a function of an implementation-defined mode-count / degrees-of-freedom proxy. Across the explored settings, the proxy remains controlled and does not exhibit unstable growth.

## 5.1 From residual proxy to an effective constant term

The vacuum module produces a residual proxy $\Delta E(\theta)$ (Eq. (10)) or an implementation-defined equivalent recorded in the Phase II run artifacts. To drive a cosmological background test, we map this residual into an effective vacuum-density proxy $\rho_\Lambda(\theta)$ using a fixed conversion in code units (held constant across all Phase II runs for auditability). We then define

$$\Omega_\Lambda(\theta) \;\propto\; \rho_\Lambda(\theta)\,, \tag{12}$$

with the proportionality fixed by the normalization conventions of the FRW integrator used in the Phase II engine (as recorded in the configuration referenced by Appendix 8).

**Scope note.** This mapping is *not* claimed to be an EFT matching or a physically derived relation between $\varepsilon$ and a physical vacuum density; it is a transparent operational embedding whose purpose is to test whether the residual proxy can be carried as a smooth constant term without numerical failure of the background module.

## 5.2 FRW integration protocol

We integrate a flat FRW system in normalized units,

$$H^2(a) \;=\; \frac{\Omega_r}{a^4} + \frac{\Omega_m}{a^3} + \Omega_\Lambda(\theta)\,, \tag{13}$$

with fixed background parameters $(\Omega_r, \Omega_m)$ chosen by configuration. The Phase II integrator evolves the system according to its configured independent variable (time or scale factor) and records the corresponding trajectory outputs; Fig. 5 plots the staged trajectory product produced by the Phase II build (see Appendix 8 for the exact run and script entry point). We compare two trajectories integrated over the same interval with identical numerical settings:

11

1. **Reference:** a baseline trajectory with $\Omega_\Lambda$ set to the reference value used by the Phase II engine (often 0 in the toy setup, or a fixed baseline).

2. **Axiom-driven:** a trajectory with $\Omega_\Lambda(\theta^\star)$ set by the mapped residual at the anchored phase $\theta^\star$.

Here $\theta^\star$ is treated as an externally supplied anchor (Phase II does not derive it); its role is to test coherent propagation of a single phase input through the pipeline.

## 5.3 Result: smooth and stable trajectories under the mapped term

Figure 5 shows that introducing $\Omega_\Lambda(\theta^\star)$ derived from the Phase II residual proxy changes the FRW trajectory relative to the reference run. Within the explored regime, the evolution remains smooth and stable: runs complete without integrator failure attributable to the mapped term, and the output trajectory exhibits no discontinuities or stiffness-driven breakdown under the configured settings. Within Phase II scope, this establishes the minimal end-to-end viability criterion: the axiom-driven residual proxy can be carried into the background module under a fixed mapping without breaking the computational chain.

## 5.4 Interpretation boundaries

Claim C2.3 is a pipeline *consistency* test, not a cosmological prediction. Specifically:

- We do not claim the Phase II normalization matches the observed cosmological constant.

- We do not claim a derived physical relation between $\varepsilon$ and $\rho_\Lambda$.

- We do claim that, under a fixed and auditable mapping, the residual proxy functions as a smooth constant-term input to the configured toy FRW integrator in the explored regime.

**Non-claims boundary (C2.3).** This result does *not* validate the mapping as physically correct, does *not* fit cosmological datasets, and does *not* establish late-time acceleration in the real universe. It supports only the bounded statement that the Phase II residual proxy can be embedded into the configured FRW background module as a constant contribution without inducing numerical failure in the explored regime, with full provenance given by Appendix 8.

# 6 Reproducibility and provenance

Phase II is designed to be reproducible from a clean repository checkout in the following operational sense: every figure included in this paper is generated from version-controlled code and an explicit configuration, and each figure is traceable to recorded run artifacts (including code-state identifiers) sufficient for independent auditing and regeneration. This section specifies (i) what is treated as authoritative, (ii) how artifacts are traced from the manuscript back to runs, and (iii) how a third party rebuilds the figures and the PDF.

## 6.1 Canonical claim-to-artifact mapping

A compact claim-to-artifact index (Claims C2.1–C2.3 $\rightarrow$ figure files, `run_id` sidecars, and run folders) is maintained in `phase2/CLAIMS.md`. For each main-text figure, the Appendix run manifest (Appendix 8) provides the `run_id` pointer(s) and the primary script/config entry point(s). These two files are the intended audit anchors: starting from any claim or figure, a reader can locate the corresponding run signature and reproduce (or at minimum verify) the artifact.

## 6.2 Repository layout and authoritative artifacts

The Phase II deliverable is structured as:

- `phase2/paper/`: the LaTeX sources of the manuscript and submission staging directory.

- `scripts/`: executable entry points that generate intermediate data products and figures.

- `config/`: configuration files specifying numerical parameters used in the runs.

- `outputs/`: generated run folders, intermediate data products, and canonical figures (treated as build artifacts).

- `Snakefile`: the deterministic build graph used to regenerate figures and compile the PDF.

**Authoritative vs. staged.** The canonical computational products live under `outputs/` (not under the paper directory). Figures included in the manuscript are staged under `phase2/paper/figures/` for arXiv-style packaging, and each staged figure is paired with a `run_id` pointer that links back to the authoritative run artifacts under `outputs/`.

## 6.3 Figure-to-run mapping, run folders, and code-state identification

Each figure in the main text corresponds to a tagged run or sweep whose provenance is recorded in Appendix 8:

- Fig. A: representative paired free vs. constrained vacuum run (Claim C2.1).

- Figs. B–D: systematic sweeps in $\varepsilon$ and discretization/UV controls (Claim C2.2).

- Fig. E: FRW trajectory comparison driven by the anchored residual (Claim C2.3).

Each staged manuscript figure has an associated sidecar file

`phase2/paper/figures/<figure_name>.run_id.txt`

containing the `run_id` (or list of `run_id`s, for sweeps) used to generate that figure. A reader can then inspect the corresponding run folder(s) under

`outputs/runs/<run_id>/`

which include machine-readable metadata (e.g. `meta.json`) recording at minimum the code state (Git commit hash), the configuration used, and execution details needed for auditing (including seeds where applicable). This establishes the concrete audit chain: *paper figure $\rightarrow$ run_ id sidecar $\rightarrow$ run folder $\rightarrow$ recorded code/config state.*

## 6.4 Build system and exact reproduction

The reference build uses a deterministic build graph (Snakemake) and `latexmk` for compilation. From the repository root, the Phase II build target regenerates canonical figures and compiles the manuscript:

`snakemake -j 1 paper`

This target (i) executes the scripts needed to generate the canonical figures under `outputs/figures/`, (ii) stages the required figures under `phase2/paper/figures/` along with their `run_id` pointers, and (iii) compiles `phase2/paper/main.tex` to `phase2/paper/main.pdf`.

Environment requirements (Python version, required packages, and LATEX toolchain) are specified by the Phase II setup documentation in the repository (e.g. top-level `README` and/or Phase II environment files). To support independent auditing even when exact environments differ, run metadata records the code state and configuration for each figure-generating run.

## 6.5   Determinism, seeds, and paired-run discipline

Where randomized initialization is used, seeds are explicitly set via configuration and recorded in run metadata. For all main-claim evidence, we employ a paired-run discipline: constrained and free baselines share identical initialization and numerical settings, differing only by enforcement of the axiom floor. This isolates the causal impact of the axiom implementation from stochastic variance and from unrelated numerical settings.

## 6.6   Data availability

All data products necessary to reproduce the plots are either:

- stored under `outputs/` as build artifacts and run folders, or

- regenerable from version-controlled code and configuration using the build command above.

The manuscript does not rely on external proprietary datasets.

# 7   Limitations and scope boundaries

This paper is intentionally claim-bounded. Phase II establishes an auditable *pipeline fact*: a strict global floor on a chosen diagnostic amplitude can be implemented stably in a minimal vacuum testbed (Claim C2.1), remains well-behaved under systematic numerical controls (Claim C2.2), and can be embedded into a toy FRW module without instability under a transparent mapping (Claim C2.3). The purpose of this section is to state precisely what these claims do *not* imply, what would falsify them, and what additional work is required before any physical interpretation can be elevated beyond the present scope.

## 7.1   Algorithmic constraint, not a derived physical law

The Origin Axiom is enforced here as an *algorithmic rule* (Sec. 2), implemented as a hard inequality on a global diagnostic amplitude with a uniform correction when violated. Phase II does not derive this constraint from a local action, does not propose a microscopic mediator, and does not claim equivalence to a known symmetry or conservation law. Accordingly, the results should be read as statements about the behavior of the specified constrained numerical system, not as a validated modification of quantum field theory.

## 7.2   Testbed status and model dependence

The vacuum sector used here is a controlled lattice testbed selected for auditability and for exhibiting near-cancellation of a global mode in the unconstrained baseline. We do not claim that the chosen scalar-field implementation is a faithful surrogate for the full Standard Model vacuum, nor that the

residual diagnostic $\Delta E$ is uniquely determined independent of model choice. The conclusions of Phase II therefore concern *existence, stability, and controlled scaling* of the constrained mechanism in this representative class of models.

## 7.3 No continuum-limit proof and limited universality

Although Claim C2.2 performs sweeps over discretization and UV-control parameters, these are not a proof of a continuum limit, renormalization-group invariance, or universality with respect to discretization scheme. In particular, percent-level stability across the explored ranges does not guarantee asymptotic stability at arbitrarily large mode counts, arbitrarily small lattice spacings, or alternative integrators/potentials. A stronger universality statement would require (i) explicit convergence tests under well-defined refinement limits and (ii) demonstration that the residual diagnostic behaves consistently under controlled changes of discretization scheme.

## 7.4 Energy accounting and interpretation

Because the enforcement step modifies only the zero mode, it can inject or remove a small amount of energy relative to the unconstrained baseline. Phase II measures this effect via paired runs; it does not assert that the constrained dynamics conserve the same Hamiltonian as the unconstrained system. Therefore, Phase II does not interpret the residual as a conserved physical vacuum energy in the QFT sense; it treats it as an operational diagnostic induced by the constraint in the chosen implementation.

## 7.5 FRW embedding is a consistency test, not a prediction

Claim C2.3 maps the residual diagnostic into an effective constant contribution in a toy FRW integrator to test end-to-end pipeline consistency. This mapping is deliberately transparent and fixed across Phase II runs for auditability; it is not claimed to be an EFT matching, a derived relation between $\varepsilon$ and physical vacuum density, or a fit to cosmological data. Accordingly, Phase II makes no quantitative claim about the observed cosmological constant, and no claim that $\theta^\star$ predicts late-time acceleration in the real universe.

## 7.6 Status of the phase anchor $\theta^\star$

The parameter $\theta^\star$ is treated in Phase II as an externally supplied empirical anchor. Phase II does not derive $\theta^\star$, does not establish its uniqueness, and does not claim that it must be associated with a Standard Model phase. The only Phase II question is whether a single phase parameter can be propagated through the pipeline without instability and with controlled, auditable dependence in the residual diagnostics.

## 7.7 What would falsify the Phase II claims

Within the scope of this paper, the following outcomes would directly undermine Claims C2.1–C2.3:

- **Non-reproducibility:** inability to regenerate the figures and PDF from the recorded run identifiers and scripts (Appendix 8 and Sec. 6).

- **Numerical pathology:** evidence that the constrained system exhibits uncontrolled blow-up, stiffness-induced failure, or strong sensitivity to minor numerical changes in the explored regime, contradicting Claim C2.2.

- **Discretization instability:** emergence of runaway scaling in the residual diagnostic as discretization controls are varied within the sweep domain claimed in Figs. B–D.

- **FRW failure under fixed mapping:** instability or pathological trajectories in the FRW module when driven by $\Omega_\Lambda(\theta^\star)$ under the stated mapping and integration settings (Claim C2.3).

## 7.8 Required upgrades for post-Phase II physical interpretation

To move beyond Phase II, additional work is required before interpreting the constraint as a viable physical principle:

- **Mechanism upgrade:** a candidate local formulation or symmetry principle whose constrained dynamics reproduce (or justify) the operational floor.

- **Universality upgrade:** controlled convergence/refinement studies and cross-implementation checks showing that the residual behavior is not an artifact of a particular discretization or integrator.

- **Mapping upgrade:** a physically motivated normalization from residual diagnostic to an effective stress-energy contribution, with dimensional analysis and calibration against known limits.

- **Model upgrade:** demonstration in richer field content (or a theoretically justified effective model) that retains the claimed stability properties.

Phase II should therefore be read as a rigorous *engineering and auditing milestone*: it demonstrates a stable constrained-cancellation mechanism and a reproducible pipeline that can be independently verified. It is not, by itself, a completion of the cosmological-constant problem or a validated fundamental theory.

# 8 Conclusion

Phase II of the Origin Axiom program was designed as a bounded, auditable test: if one enforces a strict global non-cancellation floor in a minimal vacuum testbed, does a stable residual emerge; is it robust under controlled numerical variations; and can it be carried through a transparent toy embedding into a cosmological background module without instability? Within the explicit scope boundaries stated in Sec. 7, the answer is yes.

We organized the paper around three claims and corresponding evidence:

- **Claim C2.1 (Existence under constraint).** Enforcing the hard floor $|A| \geq \varepsilon$ in the Phase II lattice vacuum testbed yields a persistent nonzero residual diagnostic relative to the matched unconstrained baseline, without numerical pathology (Fig. 1).

- **Claim C2.2 (Robustness under controls).** Across systematic sweeps in the floor scale $\varepsilon$ and discretization/UV-control parameters, the induced residual remains well-behaved and exhibits smooth, non-explosive dependence in the explored regime (Figs. 2–4).

- **Claim C2.3 (End-to-end consistency in a toy FRW module).** Under a fixed and explicitly stated mapping from the residual diagnostic to an effective constant contribution $\Omega_\Lambda(\theta)$, FRW trajectories show modest, smooth deviations without pathological behavior, demonstrating pipeline consistency rather than a cosmological prediction (Fig. 5).

A secondary Phase II objective was to test whether the pipeline can coherently carry a single phase input without instability. Treating $\theta^\star$ as an externally specified anchor (not derived in Phase II), we propagated it through the vacuum and FRW modules and observed that residual diagnostics can carry a small, structured phase dependence while remaining numerically stable. In Phase II this phase dependence is reported as an operational feature of the implemented pipeline, not as a physical identification claim.

The core contribution of Phase II is therefore methodological and reproducibility-focused: a constrained non-cancellation mechanism is specified algorithmically (Sec. 2), demonstrated to be stable in a controlled setting, stress-tested under meaningful numerical controls, and documented with end-to-end provenance so each figure can be traced to tagged runs and regenerated from a clean checkout. Reproduction instructions and repository structure are stated in Sec. 6, and per-figure run identifiers are indexed in Appendix 8.

Finally, we reiterate the boundaries. Phase II does not derive the axiom from a local action, does not claim quantitative agreement with the observed cosmological constant, and does not establish a continuum-limit theorem or uniqueness of $\theta^\star$. What it provides is a concrete, checkable baseline: a fully audited toy pipeline in which "no perfect cancellation" is imposed as a global constraint and its consequences can be measured, reproduced, and scrutinized. This establishes a stable foundation for subsequent phases to address universality, physical embedding, and stronger interpretive targets.

| Figure | Artifact stem | run_id | git |
|--------|---------------|--------|-----|
| Fig. A | figA_mode_sum_residual | figA_mode_sum_residual_20260103T124604Z | 123456789 |
| Fig. B | figB_scaling_epsilon | figB_scaling_epsilon_20260103T124609Z | 123456789 |
| Fig. C | figC_scaling_cutoff | figC_scaling_cutoff_20260103T124606Z | 123456789 |
| Fig. D | figD_scaling_modes | figD_scaling_modes_20260103T124602Z | 123456789 |
| Fig. E | figE_frw_comparison | figE_frw_comparison_20260103T124607Z | 123456789 |

# A Computational provenance

This appendix specifies the audit trail for every numerical result shown in the Phase II paper. Its purpose is narrow and concrete: enable an independent reader to (i) map each figure to the exact run artifacts that produced it, (ii) identify the precise code state and configuration used, and (iii) regenerate the outputs from a clean repository checkout.

## A.1 Audit path: figure → run_id → run folder

The canonical traceability path is:

1. **Figure in the PDF** (e.g. Fig. A–E),

2. **Figure sidecar** staged under `phase2/paper/figures/` with suffix `.run_id.txt`,

3. **Run directory** under `outputs/runs/<run_id>/`,

4. **Machine-readable run metadata** `outputs/runs/<run_id>/meta.json`,

5. **Code state and parameters** recorded in `meta.json` (including the Git commit hash and resolved configuration).

For multi-run sweeps, the figure sidecar records a list of `run_id`s. The mapping between figures, run identifiers, and claims is summarized in Appendix 8, which serves as the paper's primary audit index.

## A.2   Run identifiers and artifact structure

Each Phase II numerical execution is assigned a unique `run_id` and writes its outputs under:

`outputs/runs/<run_id>/`

A run directory contains, at minimum:

- `meta.json`: provenance metadata (code state, configuration, and execution identifiers);

- run logs (stdout/stderr or equivalent);

- raw numerical outputs and/or intermediate data products used to build figures.

**Provenance fields recorded in `meta.json`.**   For auditability, the run metadata records (directly or via explicit pointers):

- the Git commit hash identifying the exact code state used for the run;

- the resolved configuration parameters (including $\varepsilon$, discretization/UV controls, and any scan ranges);

- the `run_id` and an execution timestamp;

- any random seeds used (if randomized initialization is enabled);

- the entry point or script name used to generate the run.

## A.3   Figure sidecars and direct traceability

Every figure included in the manuscript has an associated sidecar file:

`phase2/paper/figures/<figure_name>.run_id.txt`

This sidecar records the `run_id` (or list of `run_id`s) used to generate that figure. It therefore provides a direct, file-level link from the staged manuscript figure to the authoritative run artifacts under `outputs/runs/`. Canonical figure files are generated under `outputs/figures/` and then staged for submission under `phase2/paper/figures/`.

## A.4   Regeneration via the build graph

All figures and the final PDF are generated via a deterministic build graph implemented using Snakemake. The canonical target:

`snakemake -j 1 paper`

(i) regenerates numerical outputs under `outputs/`, (ii) rebuilds canonical figures under `outputs/figures/`, (iii) stages submission figures under `phase2/paper/figures/`, and (iv) compiles `phase2/paper/main.tex` via `latexmk`. No figure appearing in the paper is generated manually or edited outside this build process.

## A.5    Paired-run discipline

For all main-claim evidence (Claims C2.1–C2.3), results are obtained using paired runs: a constrained run enforcing the Origin Axiom floor is compared against an unconstrained baseline with identical initialization, numerical parameters, and (where applicable) random seed. This isolates the causal effect of the enforcement rule from stochastic variation and unrelated numerical settings.

## A.6    Scope of reproducibility

The guarantees described here apply strictly to the Phase II implementation and to the claims as stated in the paper. They ensure that the numerical evidence presented is transparent, auditable, and reproducible. They do not imply a continuum-limit result, a unique physical interpretation of the residual, or a derived connection to observed cosmological parameters.

# References

[1] Steven Weinberg. The cosmological constant problem. *Reviews of Modern Physics*, 61(1):1–23, 1989.

[2] Sean M. Carroll. The cosmological constant. *Living Reviews in Relativity*, 4(1):1, 2001.

[3] Planck Collaboration. Planck 2018 results. vi. cosmological parameters. *Astronomy & Astrophysics*, 641:A6, 2020.

[4] Scott Dodelson. *Modern Cosmology*. Academic Press, 2003.

[5] Barbara Ryden. *Introduction to Cosmology*. Cambridge University Press, 2 edition, 2017.

FRW response to OA residual (standard FRW; explicit mapping)

Ωr=0
residual_constrained=1.86406
factor(residual→ΩΛ)=0.27
cap_mode=closure
ΩΛ,eff=0.503298
Ωm,eff=0.496702
Ωm,obs=0.3
ΩΛ,obs=0.7
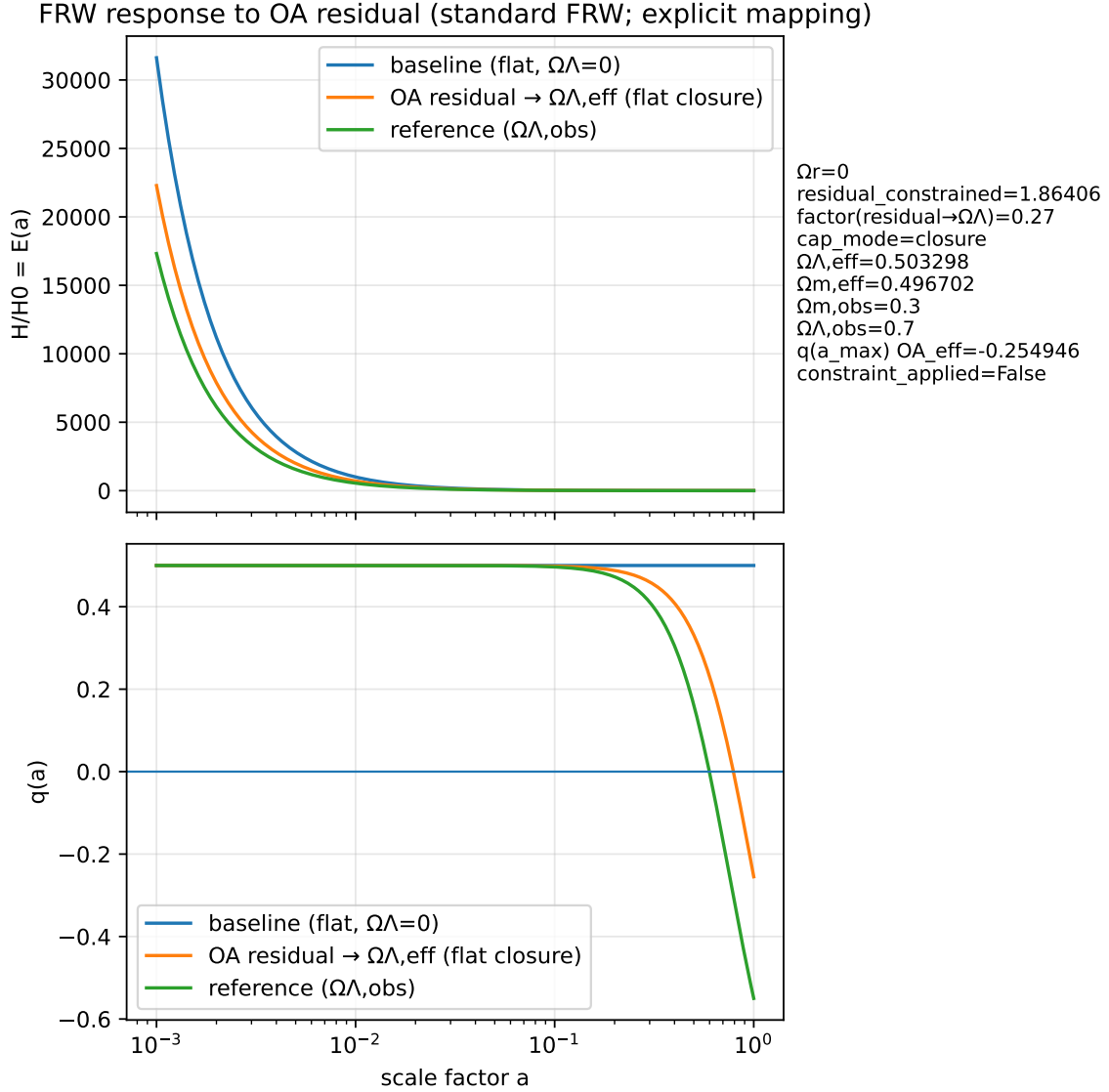q(a_max) OA_eff=-0.254946
constraint_applied=False

Figure 5: **Claim C2.3 evidence: FRW consistency under an axiom-driven constant term.** Comparison of the FRW trajectory output produced by the Phase II engine for a reference run and an axiom-driven run using $\Omega_\Lambda(\theta^\star)$ obtained from the Phase II residual proxy under the stated fixed mapping. In the explored regime, the trajectories remain smooth and numerically stable (runs complete without integrator failure), indicating that the residual proxy can be embedded as an effective constant contribution without numerical breakdown of the toy background module.